Morphology of Polyvinylidenefluoride and the Copolymer of Tetrafluoroethylene with Ethylene Using Thermomechanical Analysis

Yu. A. Olkhov,[1] S. R. Allayarov,[1] T. A. Konovalova,[2] L. D. Kispert,[2] D. E. Nikles[2]

[1]*Institute of Problems of Chemical Physics of the Russian Academy of Sciences, Chernogolovka, Moscow, Russia 142432*
[2]*Department of Chemistry, The University of Alabama, Tuscaloosa, Alabama 35487-0336*

Received 19 July 2006; accepted 4 November 2007
DOI 10.1002/app.27811
Published online 4 February 2008 in Wiley InterScience (www.interscience.wiley.com).

ABSTRACT: The morphology of polyvinylidenefluoride (PVDF) and the copolymer of tetrafluoroethylene with ethylene (CTE) were investigated by thermomechanical analysis. Both granules and highly dispersed powders of the polymers have similar morphology. Polymer granules contain amorphous and crystalline regions. The morphology of the polymer powders were determined under two analytical conditions: coaxial, when the vectors of polymer loading and vector of compression pressure are in the same plane, or when they are perpendicular to each other. One amorphous and two crystal blocks were found at coaxial orientations of the vectors. Thermomechanical analysis showed that the polymers had a completely amorphous diblock morphology at the perpendicular orientation of the vectors. Parameters that characterize a degree of interchain interaction, such as coefficients of thermal expansion, free volume, and temperatures of polymer transformation into the glassy, high-elastic, or flow-viscous state were determined. PVDF and CTE have similar topographic composition, but different molecular mass and temperatures of phase transitions. © 2008 Wiley Periodicals, Inc. J Appl Polym Sci 108: 2085–2094, 2008

Key words: polyvinylidenefluoride; copolymer of tetrafluoroethylene with ethylene; thermomechanical analysis; topological structure; molecular morphology

INTRODUCTION

It has been shown that during gas-phase prefluorination of homogeneous films and membranes, the rate of fluorinated layer formation is limited by the ability of fluorine to penetrate through the fluorinated polymer layer to the layer of the initial polymer.[1] The layers of fluorinated and initial polymer are separated by a narrow domain where major chemical reactions take place. In addition to the fluorine diffusion rate, other molecular topological characteristics, such as the phase condition of the fluorinated polymer, can affect low-temperature fluorination of polymers.

Recently, direct fluorinations of PVDF and copolymer of tetrafluoroethylene with ethylene (CTE) by molecular fluorine at 35–300 K were reported in Ref. 2. The reaction of CTE or PVDF with fluorine at low temperatures results in the abstraction of hydrogen leading to the formation of radicals which were detected at 35 K. The radical concentration produced by fluorination of CTE at 77–200 K is 10 times greater than that of the PVDF radicals formed under similar conditions due to differences in the C—H bond energies.[2] In addition, PVDF has only slightly more fluorine after fluorination with the difference below the accuracy of the energy dispersion microscopy method (1%). However, we note that radical centers are formed which suggests that some fluorine has been added. In contrast, the fluorine content in CTE increases by $\sim 3\%$ on direct fluorination.[2]

The PVDF and CTE polymers differ in how the $—CH_2—$ and $—CF_2—$ groups alternate. In PVDF, the $—CH_2—$ and $—CF_2—$ groups alternate so that every $—CH_2—$ is between two $—CF_2—$ groups, whereas in CTE, two $—CH_2—$ groups are found between the two $—CF_2—$ groups. We propose that PVDF and CTE fluorination depends on their molecular-topological structure. In spite of wide use of these polymers,[3,4] the influence of the $—CH_2—$ and $—CF_2—$ groups on their chemical activity has not been investigated. Relevant literature data[3,4] of the molecular-topological structure of these polymers are unfortunately also quite conflicting.

An important characteristic of the polymers is their molecular mass (MM). The MM together with the macromolecule chemical structure defines the physical, chemical, and mechanical properties of the polymers. The topological structure of the polymers

Correspondence to: S. R. Allayarov (sadush@icp.ac.ru).
Contract grant sponsor: Cooperative Grants Program of the U.S. Civilian Research and Development Foundation; contract grant number: RUC2-2287-CG-06.

further defines its properties. Usually, the polymer topological structure combines a wide number of parameters, such as the macromolecule structure (linear, network (crosslinked), branched) and the interchain behavior (temperature of transformation, linear thermal expansion, free volume). The temperature intervals of the polymer phase (glassy, rubber-like, and viscous-fluid) transitions are also included in defining the properties of the polymers.

In the case of many polymers, the majority of the molecular-topological parameters can be defined by classical methods of polymer structural analysis, such as DSC, X-Ray, NMR, and etc. The polymer MM and molecular mass distribution (MMD) are determined by gel permeation chromatography.[5] Other existing methods defining polymer molecular heterogeneity are based on the use of diluted solutions of linear polymers, and by examining the swelling process of the network structure of the polymers. However, some perfluorinated polymers are not easily dissolved. Therefore, their MM are determined with indirect methods[3,4] beginning with the heat treatment of the samples. This leads to the thermodestruction of the polymer which decreases its MM.

Thermomechanical spectroscopy (TMS) is a new technique of thermomechanical analysis that has been developed[6,7] for determining complex polymer molecular morphology. It is based on polymer measurements of sample deformation under a load as a function of temperature. TMS is used to identify the molecular-topological structure of polymers and polymeric compositions.[8] It permits a determination of the molecular mass characteristics of linear low soluble polymers,[8] polyblock amorphous and crystal systems,[9] polymeric compositions with interacting and inter penetrating polymeric grids,[10] and rubbers of various composition and structure.[10] Recently, the TMS method was used successfully by us to investigate the effect of radiation on the molecular-topological structure of polytetrafluoroethylene.[11]

Below are listed the experimentally[6,7,12] obtained analytical measurements using the TMS procedure:

- MMD of oligomers and polymers of various MM and chemical structures of a chain, including low soluble or practically insoluble polymer;
- MMD and its parameters of block copolymers, components in a mixture of polymers differentiated by cohesive interchain energy interactions;
- Quantitative composition of block copolymers, components in polymer blends and polymeric compositions with mineral filler;
- MMD polymeric binding compositions containing various mineral, organic and inorganic fillers, and other nonpolymeric additives;
- Quantitative distribution between topological and chemical clusters;
- Quantitative composition of components of interpenetrating and polyinter-penetrating polymeric grids;
- Quantify the crystal phase in polymers of various compositions.

In the present study, the morphology of the PVDF polymer and the CTE copolymer were investigated by TMS. A review of the methodology used[6,7,12] is described below.

METHODOLOGY

The x-y recorder is used to record two functions: deformation as a function of time and temperature as a function of time, necessary for construction of the thermomechanical curve (TMC) in coordinates of thermal expansion versus temperature. The thermomechanical analysis is performed until the temperature reaches the established molecular flow in the case of linear polymers, or the beginning of thermal degradation of a network for tailored polymers.

TMS is based on two fundamental properties of polymer macromolecules placed in a variable temperature profile. First, to perform a segmental relaxation of macromolecules in strict accordance with the methods described in Ref. 13. It assumes a monatomic increase in the MM of the polymer homologues (same MM but different geometrical structures) according to the equation:

$$\log M_i = \log M_o + A\Delta T/(B + \Delta T), \qquad (1)$$

where M_i is the MM of the polymer homologue, M_o is the Kun segment (threshold MM between a polymer and a compound), ΔT is the temperature range between a glass transition (T_g) and the fusion (T_f) temperature, A and B are constants.

Second, the deformation jump, proportional to the weight fraction of the homologues in the polymer, occurs at a particular temperature in a loaded polymer due to thermal degradation of the physical network and a decrease of the elastic modulus, E_i in the polymer. Thus, for a polymer placed in a variable temperature profile, equilibrium deformation jumps occur. The area under the TMC represents a transition band of the polymer.[14–16]

In the temperature range T_g–T_∞ all polymer macromolecules exist under a condition of flow and accompanying deformation jumps. The temperature T_∞ (temperature when high-elasticity becomes a plateau) corresponds to the flow condition for the homologue with the highest MM. Above this temperature, a process of molecular flow occurs for linear polymers, and the occurrence of a high-elasticity plateau for network polymers. This thermomechani-

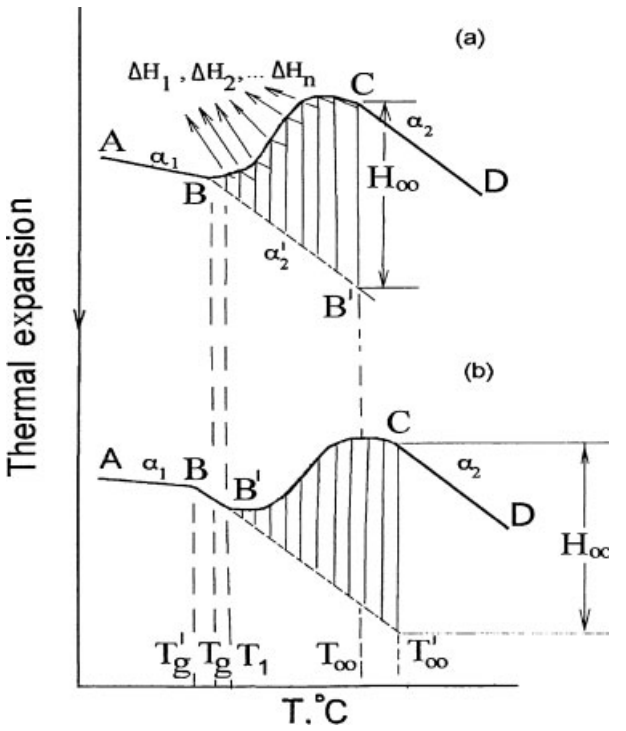

Figure 1 Thermomechanical curves of network polymer at Kun (a) and above Kun (b) values of interchain homolog.

cal behavior is a basic difference between linear and network polymers. Using the parameters of TMCs proportional to the weight fraction φ_i as the Y axis and MM M_i as X axis, the homologue transition area TMC of both network and linear polymers is a pseudointegrated curve of MMD of the analyzed polymers. The word pseudo is used when MM is determined by TMS.

The principle of thermomechanical deformation equilibrium in the transition area is basic for all polymers without an exception.[17] Therefore, analysis of thermomechanical measurements for any polymer begins with identification of the temperature range for three basic conditions of the polymer—glassy, rubbery, and viscous-flow. If a polymer contains a crystal fraction, a similar procedure should be carried out.

In network and pseudonetwork polymers the transition area of the TMC is unequivocally identified for the majority of them. A pseudonetwork is a physical network in which the thermostability of the branching junctions of the network is below the least stable chemical bonds of the polymer chain. Figure 1 shows the temperature range between T_g and T_∞. The relaxation transition of the second type is identified for the majority of TMC of network or pseudonetwork polymers by a change of deformation rate with increasing temperature in the glassy state (curve AB). The rate of the expansion deformation in this region is characterized by a linear thermal expansion factor, α_1. Thus, two types of TMC are possible. The first most widely distributed type (curve a) is characterized by the process of thermomechanical deformation which begins at the temperature corresponding to point B. It has a minimum MM at the temperature T_1. When it is in a deformation jump H_1, it is characterized by the Kun segment. At any temperature, the Ti position of the probe on the surface of the polymer is determined by two deformation processes—thermal expansion and deformation of penetration due to a decrease of the modulus of the network. It is necessary to perform their quantitative separation because the thermomechanical deformation provides the information on MM and a MMD of network polymers. For this purpose we have to compare the thermomechanical and the dilatometry curves on a straight line of expansion in the field of a glassy state (curve ABB^I). The straight line of high-elastic expansions on the dilatometry curve (line BB^I) is nearly parallel to the high-elastic plateau (line CD) on the TMC. The slope α_2^I will be a little bit greater than α_2, and the difference between them should compensate the change in the modulus of the network from temperature C to temperature D, because the cross-link yield in this range of temperatures remains invariant. In practice, the dilatometry straight line BB^I for the TMC type 1 can be carried out as straight line CD.

The above procedure for forming the dilatometry straight line BB^I is not necessary if we have a polymer of type 2 [Fig. 1(b)]. In networks of this type, the lowest MM of the intercentral homologue is much greater than the mass of the Kun segment. For them, thermomechanical deformation (point B^I) is found at temperatures above T_g. In this case the basic straight line will be carried out by extrapolation of a straight line for high-elastic expansions at a rate equal to the thermal expansion factor α_2.

An important aspect of the thermomechanical method for MMD analysis is determining the polymer condition when an equilibrium state is approached at point T_∞ (a plateau of high elasticity), similar to that of the polymeric network at equilibrium upon swelling in an appropriate solvent.[18] Thus, the integral deformation H_∞ at temperature T_∞ determines the size of the equilibrium modulus of elasticity, E_∞, and the corresponding magnitude of ν_e, the concentration of clusters in a polymeric network. For the hemispherical form of the tip of the probe with radius R_o between size H_∞ and the appropriate structural parameters, the following relationship[19] has been established:

$$E_\infty = \frac{3(1-\mu^2)P}{4R_o^{1/2} \cdot H_\infty^{3/2}}, \quad (2)$$

where μ is the Poisson ratio, and P is the load. The eq. (2) is substituted into the equation in high-elasticity theory:

$$\nu_e = \frac{E_\infty}{3RT_\infty} \tag{3}$$

in which ν_e is the concentration of inter central chains of a network in mol cm^{-3}, R, the gas constant, T_∞, the temperature where a value for a high elasticity plateaus is obtained. Having substituted eq. (3) into the expression $\overline{M}_g = d/\nu_e$ where d is the density of the polymer, we obtain the following equation for calculating the concentration of chemical junctions of a network polymer:

$$\overline{M}_g = \frac{4R_o^{1/2} \times H_\infty^{3/2} \times RT_\infty d}{(1-\mu^2)P}. \tag{4}$$

It is natural that the sum will be the size equilibrium, which is experimentally observable in practice. Having shown that

$$\overline{M}_{g_n} = \frac{1}{\sum_i^n \varphi_i / M_{g_i}} \text{ and } \overline{M}_{g_w} = \sum_i^n M_{g_i}\varphi_i. \tag{5,6}$$

where n is the number of sections with a temperature area of T_g–T_∞. Values of the weight fraction of each polymer homologue φ_i are calculated from the equation

$$\varphi_i = \frac{H_{i+1} - H_i}{\sum_i^n H_i}. \tag{7}$$

In this way we can obtain all parameters necessary for calculating $\overline{M}_{g_w}$ and $\overline{M}_{g_n}$ and for the construction of the distribution function in coordinates φ_i − log M_i.

Typical TMC for linear homopolymer and diblock copolymer behavior is given in Figure 2. Diblock copolymers may be completely amorphous or amorphous-crystal polymers.[20,21] It is necessary to attribute all polymers investigated in the present work as amorphous-crystal polymers.

We used a homopolymer as a model for demonstrating the method for calculating the molecular mass characteristics of linear monoblock polymers [Fig. 2(a)]. Such polymers, as well as network polymers, exhibit at low-temperatures, an expansion in a glassy state at constant rate (straight line AB) and are characterized by a linear thermal expansion factor α_1. At temperature B, glass transition temperature (T_g), structural relaxation of the glassy phase begins followed by segmental relaxation. It starts at the glass transition temperature (T_g). The segmental

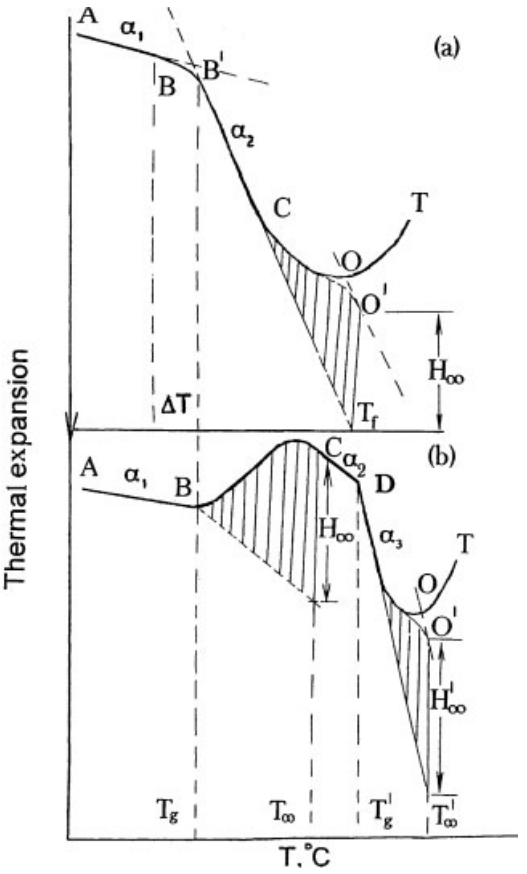

Figure 2 Thermomechanical curves of linear amorphous monoblock (a) and diblock (b) polymers.

relaxation is accompanied by expansion connected to an increase of the geometrical free volume V_f. The rate of high-elastic expansions is characterized by a linear thermal expansion factor α_2. For amorphous polymers α_1 and α_2, the threshold ratio $\alpha_2/\alpha_1 \leq 6$ has been established.[13]

The elastic region in a TMC of linear polymer continues up to temperature (C) at which the lowest MM homologue $M_{\min}$ of the polymer, changes to a condition of flow. At this point, the elastic modulus (E_1) drops and a deformation jump, ΔH, occurs i.e., the loaded hemispherical probe penetrates into the polymer, which is the softening temperature for the polymer. The magnitude of the deformation jump ΔH_1, as shown experimentally,[7] is proportional to the weight fraction of i homologues with MM $M_{\min}$. As the temperature increases the MM of the polymer-homologues increases. Accumulation of thermomechanical deforming ($H_\infty = \Delta H_1 + \Delta H_2 + \cdots + \Delta H_n$) occurs down to size H_∞ at T_∞.

However, in contrast to relaxation of the interchain central homologues in a network polymer, in which the temperature of flow for the highest MM homologue is defined unequivocally by the beginning of linear expansion in the region of high elasticity, such unambiguity is not observed in linear poly-

mers. At temperature near point O, because of the extremely small value of the modulus, the process of molecular flow begins at a temperature some degrees below T_∞. The separation procedure for components of integral deformation (curve COT) with elimination of thermomechanical deformation is described in Ref. 20. As a result of the separation, a pseudointegrated curve of MMD of linear polymer (curve CO^I) is obtained.

Calculation of the average molecular mass characteristics is reduced to dividing the temperature range T_g^I–T_∞^I by the number of temperature bands ΔT_i and to defining the general calibrating dependence eq. (1) values of M_i. Size $\varphi_i = H_{i+1} - H_i/(\sum_i^n H_i)$. Further on averaging $\overline{M}_n = 1/\sum_i^n (\varphi_i/M_i)$ and $\overline{M}_w = \sum_i^n M_i \varphi_i$; we estimate the magnitudes of the molecular characteristics and the polydispersity factor, K. Then we build the differential curve of MMD of the polymer in coordinates $\varphi_i - \log M_i$.

Let us analyze the behavior of a typical TMC linear semiblock amorphous polymer [see Fig. 2(b)]. The polymer has at least two ways to form a polyblock topological structure. The major way is the polyphilic structure of its macromolecules. Copolymers consisting of monomers with various cohesive energy usually have such a structure. Typical examples are copolymers of butadiene and styrene, or butadiene and acrylonitrile. Polymers of uniform chemical structure such as polybutadiene, polyisoprene, plant rubber, and polystyrene may also have diblock structure chains (homopolymers) because of their various isomeric and stereoisomeric composition.

Homopolymers, such as polyethylene, polypropylene, and polytetrafluoroethylene can also form polyblock topological structures. These structures can be completely amorphous and amorphous-crystalline.

The quantitative parity between regions is defined as the ratio of integral thermomechanical deformations:

$$\varphi_1 = \frac{H_\infty^I}{H_\infty^I + H_\infty}, \quad \varphi_2 = 1 - \varphi_1. \tag{8}$$

It is known from polymer physics that for an amorphous condition a certain relationship exists between α_1 and α_2 factors, namely $\alpha_2/\alpha_1 \leq 6$.[13] It is the criteria of amorphousness and crystallinity of regions in amorphous-crystalline polymers.

It was shown in Ref. 22, that upon thermomechanical analysis of crystalline polymers at the temperature of the onset of the crystal fraction melting (T_m), the expansion rate of the polymer is greater than that in a glassy state (α_2^1). The crystal fraction in amorphous-crystalline polymers is based on thermomechanical analysis, determined by estimating the integral thermomechanical deformation in the TMC transition area of the amorphous block (H_∞) and the expansion deformations upon melting of the crystalline polymer (H_k). Thus, it is necessary to take into account that in the first type, caused by penetration of the probe, that the deformation is independent of the size of the sample, but the extent of expansion upon melting of a crystal depends on the thickness of a sample. It is necessary to compare the absolute thermomechanical deformation H_∞ with the specific deformation of expansion H_k/H_o, where H_o is the thickness of the polymer sample being analyzed. The quantitative relationship between these sizes has been established[20]:

$$\varphi_{cr} = \frac{H_k/H_O}{\sum_i^n H_i}. \tag{9}$$

The values of polyblock polymer molecular mass are calculated from the equations: $\overline{\overline{M}}_n = 1/\sum_i^n \frac{\varphi_i}{\overline{M}_{n_i}}$ and $\overline{\overline{M}}_w = \sum_i^n \overline{M}_{w_i} \varphi_i$, where $\overline{\overline{M}}_n$ and $\overline{\overline{M}}_w$ are the average MM of polymer, $\overline{M}_{n_i}$ and $\overline{M}_{w_i}$ are the average MM of the macromolecule fragments in each of blocks.

EXPERIMENTAL

Materials and testing conditions

Polyvinylidenefluoride (PVDF) and the 1 : 1 copolymer tetrafluoroethylene with ethylene (CTE) were used, and their structures are shown in Scheme 1.

$$-CH_2-CH_2-CF_2-CF_2-CH_2-CH_2-CF_2-CF_2-CTE$$
$$-CH_2-CF_2-CH_2-CF_2-CH_2-CF_2-CH_2-CF_2-PVDF$$

PVDF and CTE were purchased from the Konstantinov Kirovo-Chepetsk Chemical Combine (Russia) as Fluoroplast-2 (PVDF) and Fluoroplast-40 (CTE). The amount of hydrogen in PVDF and CTE determined by elemental analysis was the same as that predicted assuming a perfect polymer of 50% each of C_2F_4 and C_2H_4 in CTE and no end group effects. NMR studies of PVDF have demonstrated that only 5–6% of the polymer is connected ''head-to-head'' consistent with other samples.[23] The degree of regular alternation of the monomers in the polymers was examined by IR spectroscopy of the CH_2 groups at 2950 and 2973 cm^{-1}, and the results were consistent with a completely alternating polymer. The granules of PVDF are truncated cylinders with a 3 mm diameter and a 4 mm length. The granules of CTE have a flat base dimension of 5 mm with a radius of 2 mm. The powders are 70 μm in size.

The thermomechanical analysis was carried out by penetration of a quartz hemispherical probe into the polymer. Dynamics of its interaction with a polymer surface is presented in Ref. 24. One of the measured

values is a change of the linear size of a sample between a substrate and the probe.

A polymer sample should have a continuous structure in the entire sample volume. It may have any shape, but it must have two plane-parallel sides separated by tens of microns up to several mm depending on the sensitivity of the measuring equipment and the temperature-expansion coefficient of the polymer.

The polymer powder of 0.2–1.0 g was compressed under the optimized pressure of 200–250 kg cm^{-2}. The DP36 press made in Germany by ''Carl Zeis Jena'' was used. The diameter of the metallic form used for pressing is 6 mm and its meets the No. 14 Russian standard for surface treatment. Pressing was carried out at room temperature. The resulting pellet was placed in the chamber of the standard thermoanalyzer ''UIP-70M'' and cooled to -100°C at a rate of 5°/min. It was maintained at this temperature for 5 min and then the probe loaded with a force of 0.5 g. Finally the sample was heated at the rate of 5°/min.

Accuracy and reproducibility of the TMS method was analyzed in Ref. 25. The accuracy of the temperature measurements in the thermostatic chamber of the instrument is $\pm 0.05^\circ$C. The accuracy of deformation is ± 5 nm. The errors of MM and free volume fraction are less than or equal to $\pm 10\%$. The data were reproducible within the error limits of ± 5 to 10%, but in some cases, it can be as large as $\pm 20\%$ due to heterogeneity of the materials and differences in their thermal and stress history.

RESULTS AND DISCUSSION

The TMCs of the CTE copolymer granules [Fig. 3(a)] and powders [Fig. 3(b,c)] tested in the coaxially and perpendicular orientation are given in Figure 3(b,c), respectively, and the TMCs for PDVF granules and powders tested coaxially are given in Figure 3(d,e), respectively.

Analysis of these curves yield α_1 and α_2, the coefficients of linear thermal expansion in the glassy and high-elasticity slate; α_k, α'_k, α''_k, the coefficients of linear thermal expansion at the fusion temperature of the low-melting, intermediate, and high-melting crystal, T_g, for the glass transition temperature of the amorphous block, T_{cl}, the glass transition temperature of a cluster, T_m, T'_m, T''_m, fusion temperature for the low-melting, intermediate and high-melting crystal modifications; T_f beginning temperature of molecular flow, T_∞ beginning temperature of a grid equilibrium state; V_f the free geometrical volume; $\overline{M}_g$ and $\overline{M}_g$ average numerical and average weight mass in a pseudo network structure of an amorphous block, $\overline{M}_n^{cr1}$, $\overline{M}_w^{cr1}$, $\overline{M}_n^{cr2}$, $\overline{M}_w^{cr2}$ the MM in the low-melting, and high melting crystal forms, $\overline{\overline{M}}_w$ average weight MM of blocks, K the polydispersity factor and φ_a, φ_{cr}, φ'_{cr}, φ''_{cr}, the weight fractions of the amorphous block, low-melting, intermediate and high-melting crystal modifications.

Topological structure of the CTE and PVDF granules

The TMC of the CTE copolymer granules, and the PVDF granules given in Figure 3(a,d), respectively, are characteristic of a polyblock amorphous-crystal structure. In the temperature range from -100 to 30°C the CTE polymer exists in a semicrystalline state and expands with temperature at a constant rate (AB line), which is characterized by a coefficient of linear thermal expansion (or contraction at cooling) $\alpha_1 = 10.64 \times 10^{-5}$ deg^{-1}.

At $T_g = 30^\circ$C the CTE copolymer shows an enhanced segmental mobility and formation of the transition area TMC, the deformation jumps ΔH_i. Deformation jumps occur in a loaded polymer because of the monotonic lowering of the physical network module upon segmental relaxation of the interchain homolog with mass M_i and weight fraction φ_i.

According to theory of[26] and thermomechanical analysis,[6,7,14,16] relaxation starts with the smallest segments (Kun segments) and ends at $T_\infty = 151^\circ$C for CTE because of the transition of the highest MM homolog into the flow state (polymer moves as a whole). The deformation jump $\Delta H_i = H_{i+1} - H_i$, corresponding to the MM M_i, is proportional to $T_i - T_g$ and allows for an estimate of the weight fraction φ_i according to the equation[27]:

$$\log M_i = 2.3 + \frac{11\Delta T_i}{100 + \Delta T_i}. \quad (10)$$

Thus, the transition area TMC of any polymer in $\varphi_i - M_i$ coordinates exists as a pseudointegral MMD curve of interlinked chains in the pseudonetwork of the amorphous block. The criterion of the topological composition of CTE is the plateau of highly elastic deformation (curve CD), where the ratio of the expansion rates in this area is $\alpha_2/\alpha_1 < 6$ ($\alpha_2 = 35.7 \times 10^{-5}$ deg^{-1}).[13]

The number–average ($\overline{M}_{g_n}$) and weight–average ($\overline{M}_{g_w}$) MM of the chain segments between junctions in amorphous regions of CTE were calculated using the program presented in Refs. 6 and 7. $\overline{M}_{g_n} = 37.2 \times 10^3$, $\overline{M}_{g_w} = 55.4 \times 10^3$, and $K_a = 1.49$, where K_a is the coefficient of polydispersity. The pseudonetwork structure of the amorphous block is formed from the crystallized fragments CTE macromolecules, which

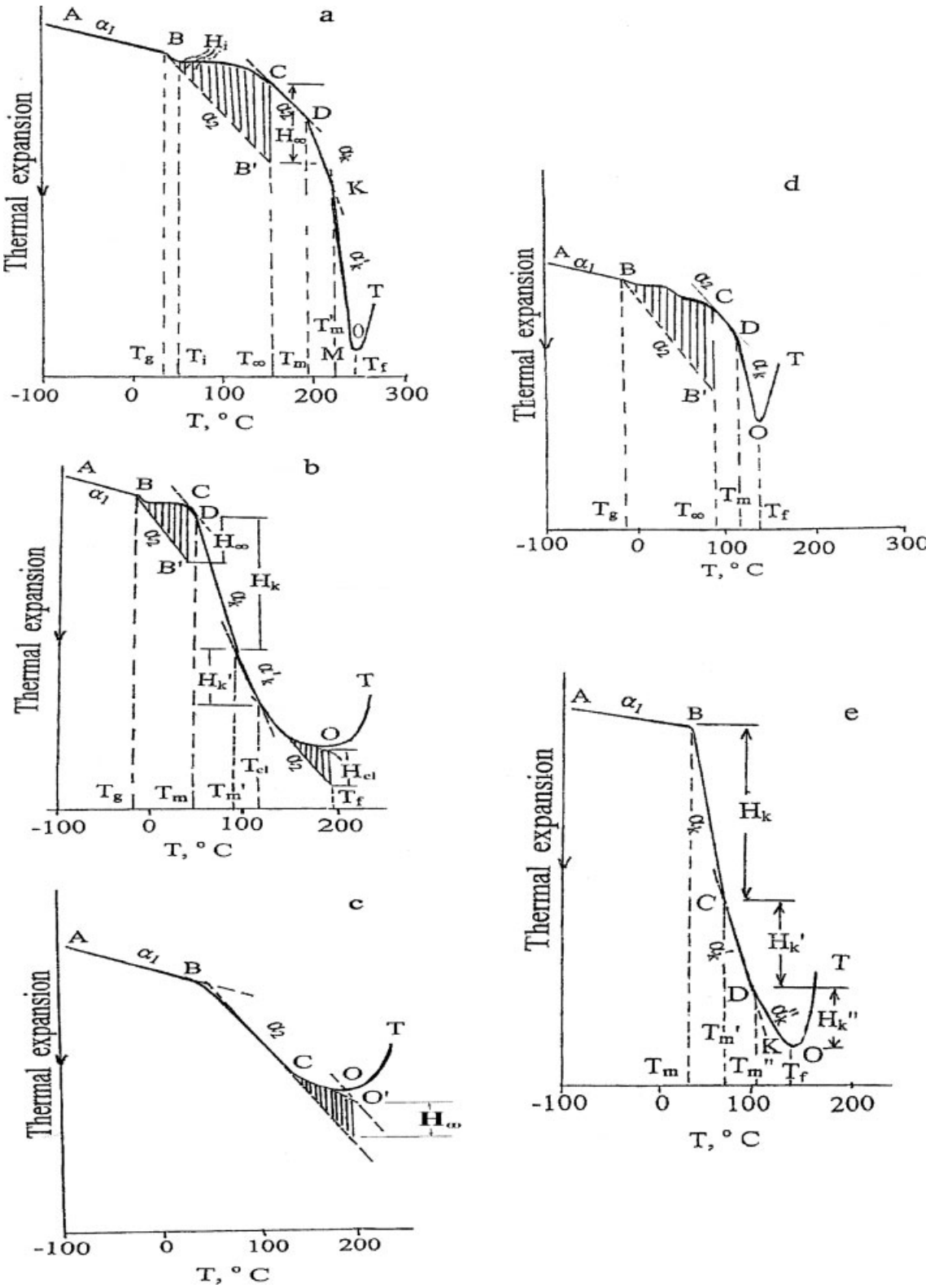

Figure 3 The TMS of granules (a,d) and powder (b,c,e) of the copolymer of tetrafluoroethylene with ethylene (a–c) and polyvinylidenefluoride (d,e). TMS tested in coaxially (b,e) and perpendicular (c) orientation of the vectors. (a) The TMS of granules of the copolymer of tetrafluoroethylene with ethylene. (b) The TMS of powder of the copolymer of tetrafluoroethylene with ethylene. TMS carried out in a coaxially orientation of the vectors. (c) The TMS of powder of the copolymer of tetrafluoroethylene with ethylene. TMS carried out in a perpendicular orientation of the vectors. (d) The TMS of granules of the polyvinylidenefluoride. (e) The TMS of powder of the polyvinylidenefluoride. TMS carried out in a coaxially orientation of the vectors.

TABLE I
Molecular and Topological Structures of the CTE and PVDF Granules

Analyzed parameters	CTE	PVDF
Amorphous region		
T_g (°C)	30	−17
T_∞ (°C)	151	87
α_1 ($\times 10^5$ deg^{-1})	10.64	6.11
α_2 ($\times 10^5$ deg^{-1})	35.7	24.7
V_f	0.228	0.143
$\overline{M}_{g_n}$ ($\times 10^{-3}$)	37.2	5.3
$\overline{M}_{g_w}$ ($\times 10^{-3}$)	55.4	7.9
K_a	1.49	1.49
φ_a	0.49	0.62
Low-melting crystalline portion		
T_m (°C)	194	105
$\overline{M}_n^{cr1}$ ($\times 10^{-3}$)	39.8	25.1
$\overline{M}_w^{cr1}$ ($\times 10^{-3}$)	39.8	79.4
K'_{cr}	1	3.16
α_k ($\times 10^5$ deg^{-1})	76.9	39.2
φ_{cr}	0.19	0.38
High-melting crystalline portion		
T'_m (°C)	220	–
$\overline{M}_n^{cr2}$ ($\times 10^{-3}$)	100.0	–
$\overline{M}_w^{cr2}$ ($\times 10^{-3}$)	100.0	–
K''_{cr}	1	–
α'_k ($\times 10^5$ deg^{-1})	109.4	–
φ_{cr}	0.32	–
T_f (°C)	252	135
Values averaged between regions[a]		
[b]$\overline{\overline{M}}_w$ ($\times 10^{-3}$)	43.3	35.1

[a]Averaging was performed using weight fractions of the regions and respective $\overline{M}_{w_i}$ magnitudes.

[b]The averaged weight molecular mass ($\overline{\overline{M}}_w$) calculated for the polyblock state of the polymers is not a true absolute value. The reason for this is that several different crystal modifications of macromolecular chains occur in the polyblock state. The $\overline{\overline{M}}_w$ calculated in the polyblock state can be used to analyze the topological structure of the macromolecules. However the absolute value of the $\overline{\overline{M}}_w$ can only be calculated for a polymer having a monoblock topological structure. The $\overline{\overline{M}}_w$ obtained in the perpendicular analysis is closer to the actual value and it will be presented below.

functions as interchain branching. Their thermostability provides the stability of the highly elastic amorphous block from $T_\infty = 151$°C to the beginning of the melting temperature of the low-melting crystal modification which occurs at $T_m = 194$°C. At $T > T_m$ the rate of the polymer expansion sharply increases as a result of the increase in polymer volume during melting.[28] The rate of expansion under stationary conditions ($\alpha_k = 76.9 \times 10^{-5}$ deg^{-1}, line DK) equals the value exceeding the barrier ratio $\alpha_k/\alpha_1 \geq 6$.[13] The MM of the low-melting crystallized fragments is calculated according to eq. (3), where ΔT is the difference in temperatures between points K and D. In the polymer studied $\overline{M}_n^{cr1} \approx \overline{M}_w^{cr1} = 39.8 \times 10^3$, and $K'_{cr} = 1.0$.

The MM of the high-melting crystallized fragments of the chain segments between junctions is calculated according to eq. (3), where ΔT is the difference in temperatures between points 0 and K. In the polymer studied $\overline{M}_n^{cr2} \approx \overline{M}_w^{cr2} = 100.0 \times 10^3$, and $K''_{cr} = 1.0$. The temperature of the beginning of molecular flow (curve OT) $T_f = 252$°C.

The weight ratio of amorphous to crystalline fragments of the chain segments between junctions of the CTE macromolecule is 0.49/0.51. The exclusive chain character of the CTE amorphous fragments with free volume $V_f = 0.228$ at T_g allows calculation of the CTE MM according to eq. (11), assuming only a single time crossing between chains of both topological blocks:

$$\overline{\overline{M}}_w = \overline{M}_{g_w}\varphi_a + \overline{M}_w^{cr}\varphi_{cr} = 43.3 \times 10^3. \quad (11)$$

The PVDF granules have the topological structure similar to that described above [Fig. 3(d)]. Parameters of the topological structure of the PVDF and CTE granules are listed in Table I.

Topological structures of the CTE and PVDF powders

Investigation of the molecular-topological structure of the polymer powders by means of TMS assumes

TABLE II
Molecular and Topological Structures of Powder of CTE and PVDF in Coaxial Orientation of Vectors

Analyzed parameters	CTE	PVDF
Amorphous region		
T_g (°C)	−18	–
α_1 ($\times 10^5$ deg^{-1})	9.43	7.8
α_2 ($\times 10^5$ deg^{-1})	31.3	–
V_f	0.167	–
K_a	1.37	–
φ_a	0.06	–
T_∞ (°C)	31	–
$\overline{M}_{g_n}$ ($\times 10^{-3}$)	3.6	–
$\overline{M}_{g_w}$ ($\times 10^{-3}$)	4.9	–
Low-melting crystalline portion		
T_m (°C)	34	35
α_k ($\times 10^5$ deg^{-1})	142.9	60.6
K_{cr}	1.08	–
φ_{cr}	0.44	0.47
$\overline{M}_n^{cr1}$ ($\times 10^{-3}$)	1,580	79.4
$\overline{M}_w^{cr1}$ ($\times 10^{-3}$)	1,700	–
Intermediate-melting crystalline portion		
T'_m (°C)	–	64.5
α'_k ($\times 10^{-5}$ deg^{-1})	–	60.0
φ'_{cr}	–	0.50
High-melting crystalline portion		
T (°C)	93 (T'_m)	106 (T''_m)
α_k ($\times 10^5$ deg^{-1})	71.4 (α'_k)	56.0 (α''_k)
K_{cr}	21.5 (K'_{cr})	4.0 (K''_{cr})
φ_{cr}	0.50 (φ'_{cr})	0.03 (φ''_{cr})
$\overline{M}_n^{cr2}$ ($\times 10^{-3}$)	300.3	6.3
$\overline{M}_w^{cr2}$ ($\times 10^{-3}$)	6,461.2	25.1
T_f (°C)	201	129
Values averaged between regions		
$\overline{\overline{M}}_w$ ($\times 10^{-3}$)	3,928.1	69.9

TABLE III
Molecular and Topological Structures of the Perpendicularly Oriented Powder of CTE and PVDF

Analyzed parameter	CTE	PVDF
Low-temperature amorphous region		
T_g (°C)	73	37
α_1 ($\times 10^5$ deg^{-1})	4.26	6.54
α_2 ($\times 10^5$ deg^{-1})	15.3	23.5
V_f	0.114	0.158
K_a	5.3	1.33
φ_a	1.0	0.69
$\overline{M}_{g_n}$ ($\times 10^{-3}$)	352.2	14.3
$\overline{M}_{g_w}$ ($\times 10^{-3}$)	1871.2	19.5
High-temperature amorphous region		
T'_g (°C)	–	56
K'_a	–	1.52
φ'_a	–	0.31
$\overline{M}_{g_n}$ ($\times 10^{-3}$)	–	1,603.5
$\overline{M}_{g_w}$ ($\times 10^{-3}$)	–	2,437.3
T_f (°C)	199	122
Values averaged between regions		
$\overline{\overline{M}}_w$ ($\times 10^{-3}$)	1871.2	769.1

their one-dimensional compression under optimized pressure [Fig. 3(b,c,e)]. In this case amorphous-crystal polymers lose their isotropic structures transforming into anisotropic ones. Because of structural changes in the polymers both the degree of crystallinity and the orientation of the crystals are changed. Some parts of the crystals become oriented perpendicular to the compression pressure vector. Thus, the vector of the compression pressure and the vector of loading during the release of the polymer deformation in the thermoanalyzer can be in the same plane (coaxial analysis) or in perpendicular planes, viz. in machine direction or parallel to stress and transverse direction or perpendicular to stress. The ratio of the degree of crystallinity ($\varphi_{cr_\parallel}/\varphi_{cr_\perp}$) determined by these two methods may be considered as a measure of structural anisotropy.

Figure 3(b) shows the TMC of the CTE copolymer measured in the temperature range from −100 to 250°C. It is characteristic of polyblock amorphous-crystal polymer coaxially oriented containing one amorphous and two crystal blocks. Parameters of their topological structures are listed in Table II.

Molecular flow of the high melting crystalline portion of the chain segments between junctions of the copolymer (curve OT) in general begins at T_f = 201°C.

Figure 3(c) shows the TMS structure which is characteristic of copolymer CTE. It is measured between 100 and 250°C with perpendicular orientation of the vectors. The plot indicates a semiamorphous topological structure. No anisotropy was detected.

Molecular and topological characteristics of the perpendicularly oriented copolymer are listed in Table III. Curves of MMD of the chain segments between junctions in a pseudonetwork of amorphous region, high-melting crystalline portion, low-temperature and high-temperature amorphous regions of CTE in coaxial and perpendicular orientation of vectors are presented in Figure 4.

The difference in average weight MM of blocks ($\overline{\overline{M}}_w$) in the coaxial (Table II) and perpendicular orientations (Table III) can be explained by the fact that several crossings of different crystal modifications by macromolecular chains occur in the coaxial orientation. Therefore, the $\overline{\overline{M}}_w$ obtained in the perpendicular analysis is closer to the actual value. Molecular flow of the polymer starts at T_f = 199°C.

Molecular topological structure of PVDF measured from −100 to 150°C and with coaxial orientation of the vectors is shown in Figure 3(e) and Table II. It is characteristic of a three-block linear polymer which is completely crystallized in the range −100 to 35°C (line AB) and has $\alpha_1 = 7.8 \times 10^{-5}$ deg^{-1}. At T = 35°C the low-melting crystal modification (Table II) begins to melt at the rate $\alpha_k = 60.6 \times 10^{-5}$ deg^{-1}. The MM of the macromolecular fragments is proportional to $\Delta T = T_g - T_f$; their weight fraction (φ_k) is proportional to H_k and equals 0.47. Intermediate and high-melting crystal modifications start to melt at the temperatures C (T'_m = 64.5°C and $\alpha'_k = 60.0 \times 10^{-5}$ deg^{-1}) and D (T''_m = 106°C and $\alpha''_k = 56.0 \times 10^{-5}$ deg^{-1}), respectively. The MM of chains of the high-melting modification (Table II) is calculated assuming a linear polymer; Melting begins at T_f = 129°C.

At perpendicular orientation of the vectors, TMS of the copolymer PVDF indicates a completely amorphous diblock structure (Table III). The average MM, 769.1×10^3, is not identical to that obtained by coaxial analysis. The topographic structure of copoly-

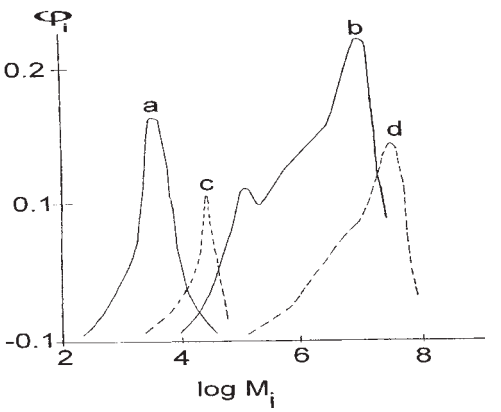

Figure 4 Molecular mass distributions of the chain segments between junctions in a pseudonetwork of amorphous region (a), fragments in high-melting crystalline portion (b), low-temperature amorphous region (c), high-temperature amorphous region (d) of CTE in coaxial (a,b) and perpendicular (c,d) orientation of vectors.

mer PVDF as well as the structures of CTE formed upon compression of powders is absolutely anisotropic.

CONCLUSIONS

Topological structures of CTE and PVDF fluoropolymers (granules or powders) were studied by the method of thermomechanical analysis. They exhibit a wide spectrum of similar parameters characteristic of the degree of interchain interactions (coefficients of linear thermal expansion, free volume, topological structure). Observable changes were found at the temperatures of the polymer conversion into the glassy, highly elastic, or viscous-flow states. Fluoropolymers PVDF and CTE have different relaxation transition temperatures. The MM is the most important parameter among PVDF and CTE characteristics. The MM along with the chemical structure of the chains defines the polymeric physical, chemical, and mechanical properties. Analysis of the results demonstrates that the CTE copolymer has a higher MM than PVDF. It is known that the rate of fluorination strongly depends on the coefficient of fluorine diffusion into the polymer matrix. Therefore, we suggest that the topological structures of PVDF and CTE greatly affect the low-temperature fluorination. These two polymers have similar topological compositions in both granules and powders but different MM and temperatures of phase transitions.

NOMENCLATURE

TMC	thermomechanical curve
α_1, α_2	coefficients of linear thermal expansion in the glassy and the high-elasticity state
α_k, α_k', α_k''	coefficients of linear thermal expansion at fusion of low-melting, intermediate, and high-melting crystal modifications
T_g	temperature of glassy transitions of the amorphous block
T_{cl}	temperature of glassy transitions of the cluster
T_m, T_m', T_m''	fusion temperatures beginning of low-melting, intermediate, and high-melting crystal modifications
T_f	temperature at the beginning of molecular flow
T_∞	beginning temperature of an equilibrium state of a grid (a high-elasticity plateau)
V_f	free geometrical volume
$\overline{M}_{g_n}$, $\overline{M}_{g_w}$	average numerical and average weight molecular mass in pseudonetwork structure of the amorphous block
$\overline{M}_n^{cr1}$, $\overline{M}_w^{cr1}$, $\overline{M}_n^{cr2}$, $\overline{M}_w^{cr2}$	molecular mass in low-melting, and high-melting crystalline modifications
$\overline{\overline{M}}_w$	average weight molecular mass of blocks
K	factor of polydispersity
φ_a, φ_{cr}, φ_{cr}', φ_{cr}''	weight fractions of the amorphous block, low-melting, intermediate, and high-melting crystalline modifications

References

1. Kharitonov, A. P.; Moskvin, Y. L.; Kharitonova, L. N.; Kotenko, A. A.; Tulskii, M. N. Kinetika i Kataliz 1994, 35, 858.
2. Allayarov, S. R.; Konovalova, T. A.; Waterfield, A.; Focsan, A. L.; Jackson, V.; Craciun, R.; Kispert, L. D.; Thrasher, J. S.; Dixon, D. A. J Fluorine Chem 2006, 127, 1294.
3. Wall, L. A. Fluoropolymers. Wiley Interscience: New York, London, Sydney, Toronto, 1972.
4. Panshin, J. A.; Malkevich, S. G.; Dunaevskaja, S. Ftoroplasti (Fluoroplastics). Khimiya: Leningrad, 1978.
5. Evreinov, V. V.; Tkachuk, Y. G.; Entelis, S. G. Vysokomol Soedin Part A 1973, 15, 4.
6. Olkhov, J. A.; Irzhak, V. I.; Baturin, S. M. RF Pat. 1,763,952 (1993).
7. Olkhov, J. A.; Irzhak, V. I.; Baturin, S. M. RF Pat. 2,023,255 (1994).
8. Olkhov, Y. A.; Belov, D. G.; Belov, G. P. J Therm Anal 1995, 46, 237.
9. Jurkowski, B.; Olkhov, Y. A.; Kelar, K.; Olkhova, O. M. Eur Polym J 2002, 38, 1229.
10. Olkhov, J. A.; Smimova, T. N.; Kotova, N. F.; Iskanov, L. I.; Milinchuk, V. K. Khim Vys Energ 1993, 27, 13.
11. Olkhov, Y. A.; Allayarov, S. R.; Chernyshova, T. E.; Barkalov, I. M.; Kispert, L. D.; Thrasher, J. S.; Fernandes, R. E.; Nikles, D. E. High Energy Chem 2006, 40, 310 (Translated from Khimiya Vysokikh Energii 2006, 40, 355).
12. Olkhov, Y. A.; Badamshina, E. R. Int J Polym Mater 1993, 19, 117.
13. Ferry, J. D. High Elastic Properties of Polymers. Wiley: New York, 1980.
14. Olkhov, Y. A.; Irzhak, T. F.; Varjuhin, S. E.; Baturin, S. M.; Irzhak, V. I. Vysokomol Soedin Part A 1997, 39, 671.
15. Olkhov, Y. A.; Irzhak, V. I. Vysokomol Soedin Part B 1998, 40, 1706.
16. Olkhov, Y. A.; Baturin, S. M.; Irzhak, V. I. Vysokomol Soedin Part A 1996, 38, 849.
17. Jurkowski, B.; Olkhov, Y. A. Thermochim Acta 2004, 414, 85.
18. Olkhov, Y. A.; Estrin, J. I. USSR Pat. 27,483 (1988).
19. Barton, J. V. Anal Proc 1971, 8, 411.
20. Olkhov, Y. A.; Jurkowski, B. J Appl Polym Sci 1997, 65, 499.
21. Olkhov, Y. A.; Jurkowski, B.; Pesetskii, S. S.; Krivoguz, M.; Kelar, K. J Appl Polym Sci 1999, 71, 1771.
22. Olkhov, Y. A.; Jurkowski, B. J Appl Polym Sci 1997, 65, 1807.
23. Wilson, C. W. J Polym Sci Ser A 1963, 1, 1305.
24. Vorovich, I. I.; Ustinov, I. A. J Appl Math Mech 1959, 23, 445.
25. Jurkowski, B.; Olkhov, Y. A. Thermochim Acta 2004, 414, 243.
26. Irzhak, V. I.; Korolev, G. V.; Solovev, M. E. Uspehi Khim 1997, 66, 179.
27. Kargin, V. A.; Slonimski, G. L. Dokl Akad Nauk SSSR 1948, 62, 239.
28. Mendelkern, L. Kristallizasiya polimerov (Crystallization of Polymers). Khimiya: Moscow-Leningrad, 1966.